

# Dilation of the oropharynx via selective stimulation of the hypoglossal nerve

Jingtao Huang<sup>1</sup>, Mesut Sahin<sup>1</sup> and Dominique M Durand<sup>2</sup>

<sup>1</sup> Center for Biomedical Engineering and Rehabilitation Science, Department of Biomedical Engineering, Louisiana Tech University, Ruston, LA 71270, USA

<sup>2</sup> Neural Engineering Center, Department of Biomedical Engineering, Case Western Reserve University, Cleveland, OH 44106, USA

E-mail: [sahin@coes.latech.edu](mailto:sahin@coes.latech.edu)

Received 4 February 2005

Accepted for publication 10 June 2005

Published 15 August 2005

Online at [stacks.iop.org/JNE/2/73](http://stacks.iop.org/JNE/2/73)

## Abstract

The functional effects of selective hypoglossal nerve (HG) stimulation with a multi-contact peripheral nerve electrode were assessed using images of the upper airways and the tongue in anesthetized beagles. A biphasic pulse train of 50 Hz frequency and 2 s duration was applied through each one of the tripolar contact sets of the nerve electrode while the pharyngeal images were acquired into a computer. The stimulation current was limited to 20% above the activation threshold for maximum selectivity. The images showed that various contact sets could generate several different activation patterns of the tongue muscles resulting in medial and/or lateral dilation and closing of the airways at the tongue root. Some of these patterns translated into an increase in the oropharyngeal size while others did not have any effect. The pharyngeal sizes were not statistically different during stimulation either between the two different positions of the head (30° and 60°), or when the lateral contacts were compared with the medial ones. The contacts that had the least effect generated an average of  $53 \pm 15\%$  pharyngeal dilation relative to the best contacts, indicating that the results are marginally sensitive to the contact position around the HG nerve trunk. These results suggest that selective HG nerve stimulation can be a useful technique to produce multiple tongue activation patterns that can dilate the pharynx. This may in turn increase the size of the patient population who can benefit from HG nerve stimulation as a treatment method for obstructive sleep apnea.

(Some figures in this article are in colour only in the electronic version)

## 1. Introduction

Obstructive sleep apnea (OSA) is an intermittent occlusion of the upper airways (UAW) resulting in frequent arterial oxygen desaturations and arousals during sleep [1, 2]. The current treatment options for OSA range from noninvasive approaches such as continuous positive airway pressure (CPAP) [3–6] to invasive surgical procedures like tracheostomy and uvulopalatopharyngoplasty (UPPP) [7]. High risk, low compliance and effectiveness, and possible side effects with such procedures limit their applications [8–10]. Currently, functional electrical stimulation (FES) of the hypoglossal nerve (HG) stands out as an alternative method of treatment.

Hypoglossal nerve stimulation has been shown to increase UAW caliber and decrease airflow resistance and compliance by activating tongue muscles [11–15].

The tongue is a structure with a large displacement in the mouth cavity and can potentially relieve the naso- and oropharynx with its forward movement [16]. The hypoglossal nerve innervates the extrinsic muscles of the tongue, i.e. the genioglossus (GG), styloglossus (SG) and the hyoglossus (HyG), the intrinsic muscles that reshape the tongue, and the geniohyoid (GH) muscle [17–19]. The activity of the GG, the fan shaped muscle underneath the tongue, is responsible for anterior positioning of the tongue, whereas the SG and HyG are considered as retractor muscles. Contraction

of GH causes anterosuperior movement of the hyoid bone [16].

The fact that the HG nerve is the main motor nerve to the tongue muscles suggests that various patterns of tongue movements should be achievable by selective stimulation of the HG nerve trunk. The main objective in this study was to investigate these patterns and to determine how they affect the pharyngeal size. The motivation is two-fold. First, the UAW anatomy varies across the human subjects. The changing response to HG nerve stimulation in human patients may be related to this anatomical variation [15]. We hypothesize that a multi-modal tongue activation paradigm has a potential to increase the patient population that can benefit from the HG stimulation as a treatment method. Second, selective stimulation can reduce the forces generated to produce the same functional output by activating only a selected subset of the muscles innervated by the HG nerve. This can in turn reduce the risk of arousing the patient from sleep and muscle fatigue during stimulations. This study tests the main hypothesis that multiple tongue activation patterns can be generated by selective HG nerve stimulation and investigates how these patterns translate into the pharyngeal size changes.

A flat-interface-nerve electrode (FINE) was used to obtain selective nerve stimulation [20]. In earlier studies, the FINE has been shown to selectively stimulate fascicles inside a nerve and activate the corresponding muscles [20–23]. This electrode produces selectivity by reshaping the nerve into a flat profile, thereby moving the fascicles closer to the stimulating contacts.

Preliminary data from this work were published in an abstract form [24].

## 2. Methodology

### 2.1. Experimental setup

Experimental protocols were reviewed and approved by the Animal Care and Use Committee at Louisiana Tech University. Seven beagles (10 kg) were used in this study. Anesthesia was induced with sodium pentobarbital ( $30 \text{ mg kg}^{-1}$ , IV) and maintained with smaller doses ( $6 \text{ mg kg}^{-1}$ , IV) of it when needed. Dexamethasone ( $0.25 \text{ mg kg}^{-1}$ ) was given to prevent edema at the start of surgery. Surgical areas were shaved and the animal was transferred to a heated-top surgery table. Rectal temperature was kept at  $38^\circ\text{C}$ . Femoral artery and vein were catheterized for monitoring blood pressure and injection of fluids. Lactated Ringer's solution was administered intravenously. Tracheotomy was performed and the animal was connected to a mechanical ventilator through the tracheal tube to suppress spontaneous breathing. End-tidal  $\text{CO}_2$  ( $<4\%$ ) and electrocardiogram were monitored.

A longitudinal incision was made over the sub-mandibular region to the left of the midline. The left hypoglossal (HG) nerve was exposed with blunt dissection. A flat-interface-nerve electrode was implanted on the HG nerve trunk immediately proximal to the bifurcation point of the distal branches occurring over the hyoglossus (figure 2). The

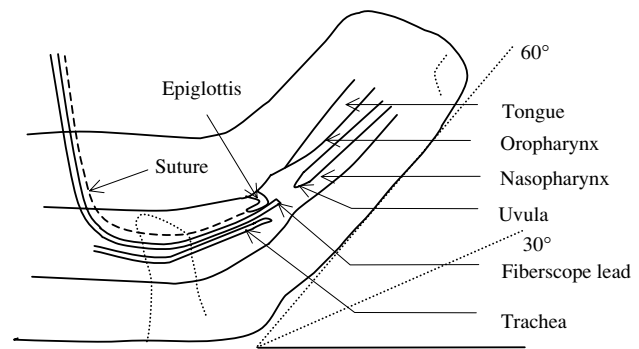


**Figure 1.** Positioning of the dog's head in  $30^\circ$  and  $60^\circ$  with respect to the horizontal plane and the fiberscope lead through the tracheal hole before the soft palate to image the oro- and nasopharyngeal openings. The epiglottis was pulled back into the trachea with a suture to clear the space in front of the camera.

implantation was done by placing the HG nerve into the electrode through the open side of the electrode and then closing with a suture, without prior knowledge of the nerve fascicle locations inside the nerve. During the implantation procedure, no effort was made to reshape the nerve manually. The electrode reshaped the nerve over the next 2 to 3 h as the electrode beams moved back to their resting position. The lead wires were connected to the stimulator through a switch box.

Cylindrical cuff electrodes were implanted onto each one of the five branches distal to the FINE (figure 2). The animal's head was fixed at an angle of either  $30^\circ$  or  $60^\circ$  from the horizontal with the mouth open or closed (figure 1). In open mouth cases, the lower jaw and the tongue were pulled up to the vertical position using rubber bands for imaging the tongue and the pharyngeal opening at its root.

A fiberscope lead (Small Animal Bronchoscope 60001VL, diam. 5 mm, KARL STORZ, Goleta, CA) was inserted cephalad through the tracheostomy hole and fixed immediately pass the edge of trachea to image the oro- and naso-pharyngeal openings (figure 1). A suture was tied to the epiglottis and pulled back into the trachea caudally to clear the opening in front of the fiberscope lead. Various angles of the fiberscope tip were tried for best viewing.

### 2.2. Stimulation and recording protocol

The electrodes of this study were fabricated using gold contacts deposited on a polyimide substrate. Two sets of contacts were molded into the geometry shown in figure 2 using a silicone elastomer (MED4-4211, Nusil Silicon Technology, Carpinteria, CA). The final FINE electrode had 16 sets of tripolar contacts positioned around the nerve trunk, 8 on the top and 8 on the bottom side of the nerve, and numbered sequentially around the nerve as shown in figure 2. The contacts 1–4 and 13–16 were referred to as 'medial contacts' and 5–12 as 'lateral contacts'. The cathodes were evenly spaced (inter-contact distance = 1 mm), and the two large, transverse contacts were shorted on each side to form a common anode (figure 2). The electrode had a window size of  $8 \text{ mm} \times 0.6 \text{ mm}$ . The cathodic contacts had an area of

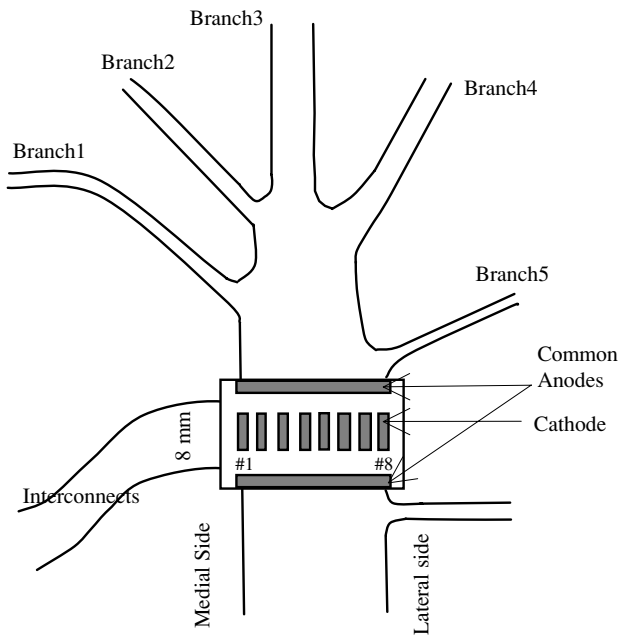


**Figure 2.** Implantation site of the FINE and branching of the HG nerve (left side). Five major branches are numbered sequentially in the medio-lateral direction. This mapping of the HG nerve branches was reproducible across the animals with minor changes. The FINE contacts 1–4 and 13–16 were referred to as medial and 5–12 as lateral contacts in the text.

$1 \times 0.4$  mm. The thickness of the walls was set to 2 mm to provide sufficient force for reshaping the nerve within a few hours.

A custom-made virtual instrument in LabView® (National Instruments, Austin, TX), a data acquisition card (NI 6071E, National Instruments) and a linear stimulus isolator (A395, World Precision Instruments) were used to generate the stimulation train. A train of charge-balanced biphasic current pulses ( $f = 50$  Hz, train duration = 2 s) of varying amplitude (0–2 mA) was applied through each one of the 16 tripolar contact sets of the FINE (one cathode and the common anodes on each side, figure 2) and the branch cuff electrodes using a switch box. Each pulse consisted of a cathodic phase of 100  $\mu$ s followed by a 100  $\mu$ s delay and an anodic phase of 400  $\mu$ s with 1/4 amplitude of the cathodic phase.

The threshold for each contact or branch was defined as the minimum current level needed to obtain visible movements of the tongue. The maximum current level was less than 20% suprathreshold, where the tongue activation pattern did not yet indicate a significant spill over to other fascicles in the nerve. Images were acquired at the threshold, the maximum, and three more levels equally spaced between the two, i.e. at a total of five different amplitudes.

The pharyngeal images were acquired into a computer using the FlashBus MV Lite (Integral Technologies, Indianapolis, IN) image grabber system; one frame before stimulation as a control and one frame a second after the onset of the stimulus train. The stimulus train was turned off after

2 s and the procedure was repeated five times for each current level.

Thus, six images were captured for each current level; one control and five stimulation images. Considering that two positions of the head (30/60°) and the mouth (open/closed) were used, the number of images collected for each contact was 120. The total number of images was 1920 for all the contacts of the FINE (120  $\times$  16) and 600 for all branches (5  $\times$  120) in an experiment. For the open mouth positions, the tongue activation patterns were viewed and recorded with a digital camcorder through the mouth along with the fiberoscopy images.

### 2.3. Data analysis

Images were loaded into Matlab® and the pixels surrounding the oropharyngeal opening were marked manually (black dots in figure 4(B), top lateral). A Matlab® code was used to calculate the cross section area enclosed by the selected pixels. For every contact, one control image and five stimulated images (one for each current level) were selected for analysis. The increase in the oropharyngeal size corresponding to the stimulus level of 10% above the threshold was calculated by interpolation. For each contact, the percent dilation in the oropharyngeal opening was found using the following equation:

$$\text{percent dilation} = \frac{A_{\text{stim}}}{(A_{\text{stim}})_{\text{max}}} \times 100 \quad (1)$$

where  $A_{\text{stim}}$  represents the oropharyngeal area at 10% suprathreshold stimulation. The maximal value of  $A_{\text{stim}}$  among all 16 contacts was denoted as  $(A_{\text{stim}})_{\text{max}}$ .

The percent opening with the best contact was compared with the best branch stimulation using

$$\text{contact versus branch} = \frac{A_{\text{contact}}}{A_{\text{branch}}} \times 100 \quad (2)$$

where  $A_{\text{contact}}$  represents the largest oropharyngeal area obtained with the best contact and  $A_{\text{branch}}$  with the best branch.

## 3. Results

### 3.1. Activation patterns in the tongue images

Transoral images demonstrated a number of tongue activation patterns. Figure 3 shows some typical patterns for 30° head position, open mouth case, which included medial (top right image) or lateral (middle left image) depression of the tongue root toward the base of the mouth. Simultaneous depression of the medial and lateral sites resulted in a large dilation of the pharynx at the tongue root (middle right image). When the current level was just above the threshold, only intrinsic muscle contractions resulting in changes of the tongue shape were observed (bottom left). For some contacts, when the stimulation current was just above the threshold, closure of the tongue root could be observed from the transoral images (bottom right). However, this closure did not translate into a decrease of the oropharyngeal opening, as determined

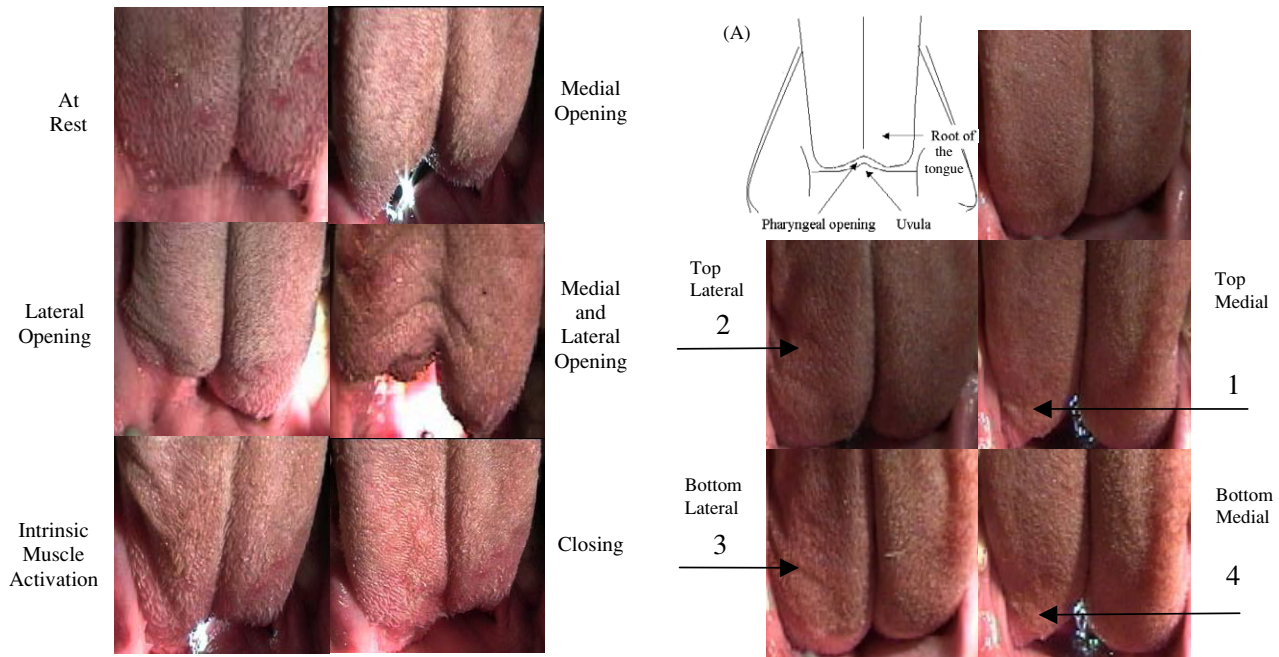


**Figure 3.** Transoral images of the tongue at rest (top left) and during FINE stimulation showing some typical tongue activation patterns, indicated by the label next to each picture. The head was 30° from the horizontal with the mouth open. See the drawing in figure 4(A) for various structures in the images. All images were taken at a stimulation current of less than 20% above the activation threshold.

by fiberoscopy images. At current levels 10% above the threshold, the activation pattern was always an opening of the oropharynx if there was any change. When the current amplitude was increased further (over 20% above threshold), the movement pattern changed as a result of current spread to other muscles, which further increased the opening at the tongue root as well as at the oropharynx.

### 3.2. Medio-lateral progression of the tongue activation pattern

Images taken in 30° head position, open mouth case in one of the beagles were selected to show typical movement modes of the tongue and the corresponding pharyngeal images observed in the same experiment (figure 4). The activation pattern of the tongue root shifted in the medio-lateral direction when the stimulation current was switched from medial contacts to lateral ones. Adjacent contacts caused similar movement patterns and transition from one pattern to the next was smooth. Stimulation through the top medial contacts (no 1–4) of the FINE stiffened the tongue longitudinally and the base of the tongue was depressed medially (figure 4(A), arrow 1). An opening at the tongue base was obtained in these cases, which translated into both left- and right-side oropharyngeal dilation (figure 4(B), top medial). Stimulation through the top lateral contacts (no 5–8) of the FINE caused the depression of the tongue muscles toward the floor of the mouth laterally (figure 4(A), arrow 2). There was a little change of pharyngeal area at the tongue root. However,

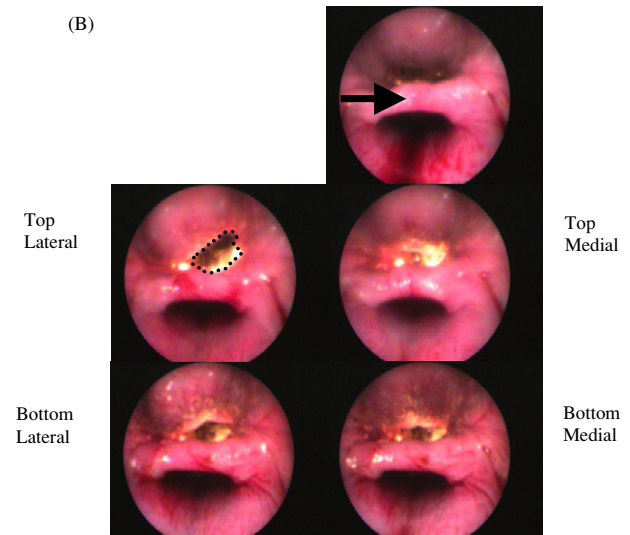


**Figure 4.** Tongue and pharyngeal images comparing the effects of medial and lateral contacts in an experiment. The head was 30° from the horizontal with the mouth open. Panel (A): top left drawing shows the relevant structures in the images. Top right: the control image at rest; the middle row: stimulation through top lateral and medial contacts of the FINE, respectively; the bottom row: stimulation through bottom lateral and medial contacts of the FINE. Panel (B): corresponding pharyngeal images to the tongue images shown in (A). The septum in the middle is the caudal end of the soft palate (the arrow). The nasopharynx is the opening below the soft palate and the oropharynx is that above (dog is in supine position). The right side in the images is the stimulated (left) side of the animal. In the top lateral image, the border of the oropharyngeal opening was marked as it was done for area measurements on the computer.

this translated into dilation on the stimulated (left) side of the oropharynx (figure 4(B), top lateral).

Stimulation through the bottom medial contacts (no 13–16) of the FINE resulted in similar activation patterns to that

**Table 1.** Comparison of medial and lateral contacts of the FINE in terms of oropharyngeal opening. Results are normalized by the dilation provided by the best contact in each experiment (see equation (1)) and averaged in each group, e.g. medial or lateral contact group ( $n = 8$  for each). Data were collected in five out of seven experiments for each position of the head ( $30^\circ$  and  $60^\circ$ ).

Exp. no	Open mouth $30^\circ$		Open mouth $60^\circ$	
	Medial contacts (%)	Lateral contacts (%)	Medial contacts (%)	Lateral contacts (%)
1	74 ± 15	53 ± 6	74 ± 15	44 ± 24
2	71 ± 17	56 ± 7		
3			85 ± 7	85 ± 7
4	91 ± 8	86 ± 6		
5			60 ± 9	59 ± 26
6	61 ± 12	64 ± 19	79 ± 11	76 ± 10
7	73 ± 8	74 ± 11	85 ± 9	78 ± 6
Paired $t$ -test	$p = 0.18$		$p = 0.22$	

**Table 2.** Comparison of the best FINE contact and the best branch stimulations according to equation (2) in each experiment. Data were collected in five out of seven experiments for each position of the head ( $30^\circ$  and  $60^\circ$ ). Percent dilations from the resting size of the oropharynx are also shown as percentages.

Exp. no	Open mouth $30^\circ$				Open mouth $60^\circ$			
	Best FINE contact number	Percent dilation from rest	Percent dilation with best branch from rest	Best contact/best branch equation (2) (%)	Best FINE contact number	Percent dilation from rest	Percent dilation with best branch from rest	Best contact/best branch equation (2) (%)
1	14	126	136	106	12	212	153	168
2	4	163	180	121				
3					11	120	131	99
4	15	124	138	89				
5					11	201	158	123
6	12	181	158	122	4	135	128	107
7	10	147	184	104	3	102	132	68
Mean ± STD		148 ± 24	159 ± 23%	108 ± 12%		154 ± 50	141 ± 14%	113 ± 33%

caused by the top medial contacts: large airway opening with depression of the medial part of the tongue (figure 4(A), arrow 4). The pharyngeal images indicate bilateral dilation of the oropharynx (figure 4(B), bottom medial).

Bottom lateral contacts (no 9–12) generated similar movement patterns to those contacts on the top lateral: depression on the lateral side without opening at the tongue base (figure 4(A), arrow 3). Oropharyngeal dilation was observed only on the stimulated (left) side (figure 4(B), bottom lateral).

This medio-lateral progression of the tongue activation pattern as the stimulation was moved from the medial to the lateral contacts was observed consistently in all animals. The medial and lateral contact stimulations were compared in table 1 in terms of the oropharyngeal dilation calculated using equation (1). There was no statistical difference between the two groups either for  $30^\circ$  head position ( $p = 0.18$ ) or for  $60^\circ$  ( $p = 0.22$ ). Therefore, the medial and lateral contacts produced the same percent dilations relative to the maximum value measured. The position of the best contacts from all experiments (listed in table 2) spread over all quadrants of the electrode with the exception of the top-lateral quadrant.

### 3.3. Pharyngeal dilation with FINE stimulation

The percent dilation of the oropharyngeal size was calculated relative to the resting size for the most effective contacts of the

FINE (best contacts in table 2) for open mouth cases in each experiment. The average of the best contacts was  $148 \pm 24\%$  ( $n = 5$ ) for the  $30^\circ$  and  $154 \pm 50\%$  ( $n = 5$ ) for the  $60^\circ$  head position. The average percent dilations obtained with all the contacts of the FINE were compared between the open mouth  $30^\circ$  and  $60^\circ$  positions of the head across all experiments; the difference was not significant (paired  $t$ -test,  $p = 0.23$ ).

For the close mouth cases, nerve stimulation enlarged the pharyngeal size only in 4 out of 10 cases (2 of  $30^\circ$  and 2 of  $60^\circ$  cases). In the remaining experiments, the oropharyngeal dilation was not detectable once the mouth was closed.

In these four close mouth cases, the best contacts were either top (two cases) or bottom (two cases) medial contacts. The percent openings with the best contacts were 137% and 89% for the  $30^\circ$  head position, and 158% and 107% for the  $60^\circ$  position, when compared to the best branch stimulation using equation (2).

The average percent dilation for the  $30^\circ$  open mouth cases ( $n = 5$ ) is plotted against the contact number in figure 5. The percent dilation values were first calculated (equation (1)), and then rank ordered from smallest to largest. The sorted data were averaged across all the experiments. The plot shows that any arbitrarily chosen contact would generate at least a dilation of  $53 \pm 15\%$  on average, relative to the best contact. However, to guarantee a minimum of 75% dilation, an arbitrarily chosen set of at least 12 contacts (out of 16) need to be used. This set of 12 contacts is guaranteed to have the contact that generates

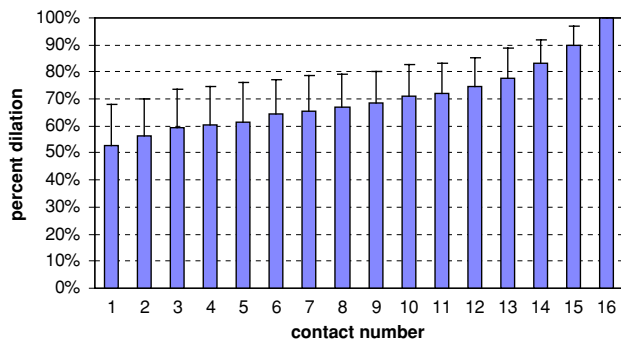


**Figure 5.** Average oropharyngeal dilation for open mouth 30° case for each contact. Normalized dilation values (equation (1)) were sorted from smallest to largest in each experiment and averaged across all five experiments. Standard deviation bars are also shown.

the 75% average dilation. This plot shows how sensitive the functional results of the HG stimulation are to the selection of the contacts.

### 3.4. Branch stimulation

There were several different tongue movement patterns observed during branch stimulation at a stimulus level of 10% above the threshold. Figure 6 shows these patterns at 30° head and open mouth position in an experiment: slight to significant closure of the region at the tongue root (branches 1 and 2); mild (branch 4) to significant (branch 3) opening; and changing of the tongue shape without opening or closing (branch 5). Those patterns were similar to those obtained during contact stimulation but not exactly the same. For both open mouth head positions, branch 3 was the most effective branch in 8 cases out of 10 (open mouth 30° and 60° in five experiments). The enlargement of the pharynx was bilateral with branch 3 (figure 6(B), middle right). Branch 4 was the second best, although the pharyngeal enlargement was unilateral (figure 5(B), bottom left). The other 3 branches did not open the pharynx significantly at 10% suprathreshold level. However, when current level was increased above 10%, the observed pattern was always a dilation with all branches.

The percent dilation of the oropharyngeal size was calculated relative to the resting size for the best branch stimulation for open mouth cases in each experiment. The average of the best branches was  $159 \pm 22\%$  ( $n = 5$ ) for the 30° and  $141 \pm 14\%$  ( $n = 5$ ) for the 60° head position (table 2).

### 3.5. Comparison of FINE and branch stimulation

The best branch and the best contact changed from experiment to experiment due to the variations in anatomy and the relative position of the electrode around the nerve. The branch and the FINE contacts that generated the maximal oropharyngeal dilation were compared using equation (2). Although the FINE stimulation did better on average in both positions of the head ( $108 \pm 12\%$  versus  $113 \pm 33\%$  in table 2), the difference was not statistically significant ( $p = 0.82$ , paired *t*-test).

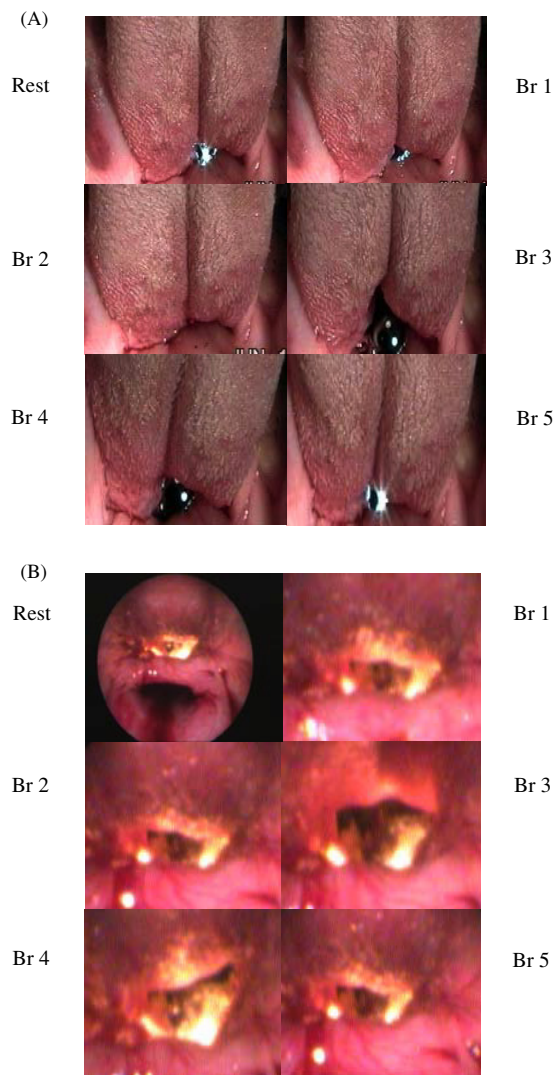


**Figure 6.** Typical images of branch stimulation taken in 30° open mouth position from one experiment (A) and the corresponding pharyngeal images (B). The stimulated branch is indicated next to the picture in the same order as shown in figure 2. The stimulus current was less than 10% above the threshold for each branch.

## 4. Discussion

Activation patterns of the tongue and the simultaneous changes in the oropharynx size were studied during selective stimulation of the HG nerve. The stimulations changed the size and the shape of the airways at the level of the tongue root in a few different modes. These were typically medial dilation, lateral dilation, closing and mere shape changes of the tongue due to intrinsic muscle activation. Each one of these activation patterns was contributed by intrinsic and extrinsic muscles at different combinations changing from one type to another as a continuum and therefore it was difficult to quantify the changes.

The HG stimulation affected only the oropharyngeal area and not the nasopharyngeal opening at the level of the soft palate, as imaged with the fiberoscopy camera. The middle and caudal portions of the nasopharynx are attached

dorsally to the base of the skull and the muscles such as the pterygopharyngeus and the palatopharyngeus constrict and draw the nasopharynx forward [16]. The ventral boundary of the nasopharynx is the mobile soft palate. The muscles of the soft palate consist of the paired palatine muscles, tensor and levator veli palatine muscles. None of the muscles responsible for reshaping the nasopharynx is innervated by the HG nerve. Moreover, the mechanical coupling between the tongue musculature and the nasopharynx is expected to be much weaker than the coupling between the tongue and the oropharynx because of the anatomy [16]. Thus, it is not surprising that the HG nerve stimulation did not affect the nasopharyngeal area. The change in the oropharyngeal size must also be due to the reshaping of the entire structure by activation of the tongue muscles, since no pharyngeal muscle was stimulated.

The way the tongue activation translates into the naso- and oropharyngeal size depends on the anatomy. In humans, nasopharyngeal size changes may be possible as a result of HG stimulation, even though we did not observe this fact in dogs. In OSA patients, the occlusions occur at the oro- or nasopharynx [25]. Thus, dilation of either one of the pharyngeal openings can benefit the OSA patients.

The FINE works on the principle that a peripheral nerve can be reshaped slowly without introducing trauma [23]. The window size of the electrode (8 mm × 0.6 mm) was chosen to reshape the HG nerve by aligning the fascicles without significantly reshaping them [21]. The observation of the explanted nerves indicated that the HG nerve was reshaped into the resting window size of the electrode. The fascicles in the middle of the nerve were closer to the contacts after reshaping as revealed by the histology (not presented). This rearrangement of the fascicles is the mechanism for selectivity. The selectivity of HG nerve stimulation with the FINE was demonstrated in a previous study [21]. Although, we did not quantify the selectivity in the current study, changes in the tongue activation patterns indicated that the selectivity was lost at current levels larger than 20%. The muscle forces increased quickly and became very large above the threshold. At larger current levels (>2 times the threshold), the tongue activation pattern was the same regardless of the contact used, indicating that the current was strong enough to activate the whole nerve. Thus, the current was limited at 20% above the threshold to achieve functional selectivity and the percent dilation (equation (1)) was calculated at 10% suprathreshold stimulus by interpolation. The current level was also limited at 20% suprathreshold for branch stimulation so that the data from contact and branch stimulation were comparable.

Electrical stimulation through the medial contacts of the FINE caused bilateral oropharyngeal opening while the lateral contacts caused openings only on the stimulated (left) side. A possible explanation is that the fibers near the medial side of the HG nerve may be cross-innervating the muscles on the contralateral side of the tongue. The opening was both in the anteroposterior and in the mediolateral direction for medial contact stimulation. For branch stimulation, only branch 3 caused bilateral oropharyngeal opening; for all other branches the dilation was on the stimulated side.

Retraction or protrusion of the whole tongue was not observed in the open mouth positions. This may be due to the fact that the stimulations were limited at 20% suprathreshold. It may also result from that the tongue was immobilized from its tip to better observe the effect of stimulations inside the pharynx.

Anesthesia reduces upper airway muscle activity significantly compared to wakefulness [26] and can even cause partial or complete airway obstruction [27]. In this study, although anesthesia alone did not completely close the airways in the beginning of the experiments, edema developed and the combined effect closed the pharyngeal opening in a few hours into the experiment. To overcome this problem, dexamethasone was administered early in the experiment, which resulted in a slightly open oropharynx at the resting state.

Spontaneous breathing was suppressed by mechanically ventilating the animal. No phasic changes were observed in the oropharyngeal size with respiration. Thus, synchronization of the stimulations with the breathing cycle was not needed to eliminate the effect of respiration in the images.

A number of reports looked at the effects of HG nerve stimulation on the UAWs using output variables such as the critical pressure ( $P_{crit}$ , nasal pressure below which airflow ceased) [13, 28], the pressure–flow relation [29, 30] and electromyography (EMG) [15, 21]. The imaging methods have been used only in a few reports [31, 32]. Pressure or flow measurements do not provide information about how the stimulation changes the upper airway morphology. The conclusions made based on these output measures may not be applicable to human subjects because of the major differences between the animal and human upper airway anatomy. With fiberoptic imaging, we were able to investigate the qualitative details of how the HG stimulation affected the tongue and the airways and thus determine if selective stimulation is a promising approach for human subjects.

Optical deformation introduced by the lenses of endoscope makes it difficult to determine the oropharyngeal opening quantitatively, especially when large angular field lenses are used. Moreover, when the plane of the object of interest is not parallel to the plane of lenses, the area measurements may not be accurate. In this study, we were only interested in relative changes in the areas measured. However, the aforementioned nonlinearity errors would remain even though the measurements are relative.

Finally, it should be noted that the implants in this study were short term. A potential complication that may arise in a long-term implant is the tissue growth between the electrode contacts and the nerve, which can affect the current pathways inside the electrode and thereby the selectivity. The results of this study should be verified with chronic implants in experimental animals.

## 5. Conclusions

Selective stimulation of the HG nerve trunk through a multi-contact electrode produced several activation patterns of the

tongue that changed the size and shape of the airways at the level of the tongue base. Some of these patterns translated into dilation of the oropharynx, some did not affect the oropharyngeal opening, and rarely caused closing (at stimulus levels near the activation threshold). The effect of the neural stimulation on the pharyngeal size was independent of the head position and marginally sensitive to the contact position around the HG nerve trunk. These results suggest that selective HG nerve stimulation can be a useful technique to obtain multiple tongue activation patterns that can dilate the pharynx. This may increase the size of the patient population that can benefit from HG nerve stimulation as a treatment method for obstructive sleep apnea.

## References

- [1] Young T B, Peppard P and Cottlieb D J 2002 Epidemiology of obstructive sleep apnea *Am. J. Respir. Crit. Care Med.* **165** 1217–39
- [2] Gislason T, Alquist M, Erikson G, Taube A and Bomem G 1988 Prevalence of sleep apnea syndrome among Swedish men: an epidemiological study *J. Clin. Epidemiol.* **61** 571–6
- [3] Faccenda J, Boon N A, Mackay T W and Douglas N J 2001 CPAP effects on blood pressure in the sleep apnoea/hyperpnoea syndrome during a randomized controlled trial *Am. J. Respir. Crit. Care Med.* **163** 344–8
- [4] Pepperell J, Ramdassingh-Dow S, Crosthwaite N, Mullins R, Jenkinson C, Stradling J R and Davies R J 2002 Ambulatory blood pressure after therapeutic and subtherapeutic nasal continuous positive airway pressure for obstructive sleep apnea: a randomized parallel trial *Lancet* **359** 204–10
- [5] Jenkinson C, Davies R J, Mullins R and Stradling J R 1999 Comparison of therapeutic and subtherapeutic nasal continuous positive airway pressure for obstructive sleep apnoea: a randomized prospective parallel trial *Lancet* **353** 2100–5
- [6] Hack M, Davies R J, Mullins R, Choi S J, Ramdassingh-Dow S, Jenkinson C and Stradling J R 2000 Randomised prospective parallel trial of therapeutic versus subtherapeutic nasal continuous positive airway pressure on simulated steering performance in patients with obstructive sleep apnoea *Thorax* **55** 224–31
- [7] Fujita S, Conway W, Zorick F and Roth T 1981 Surgical correction of anatomic abnormalities in obstructive sleep apnea syndrome: Uvulopalatopharyngoplasty *Otolaryngol. Head Neck Surg.* **89** 923–34
- [8] Hudgel D W and Auckley D H 1999 Treatment of obstructive sleep apnea *Respir. Care Clin. N. Am.* **5** 379–94
- [9] Loube D I 1999 Technologic advances in the treatment of obstructive sleep apnea syndrome *Chest* **116** 1426–33
- [10] Malhotra A and White D P 2002 Obstructive sleep apnea *Lancet* **360** 237–45
- [11] Eisele D W, Schwartz A R and Smith P L 2003 Tongue neuromuscular and direct hypoglossal nerve stimulation for obstructive sleep apnea *Arch. Otolaryngol. Clin. N. Am.* **36** 501–10
- [12] Hida W, Kurosawa H, Okabe S, Kikuchi Y, Midorikawa J, Chung Y, Takashima T and Shirato K 1995 Hypoglossal nerve stimulation affects the pressure-volume behavior of the upper airway *Am. J. Respir. Crit. Care Med.* **151** 455–60
- [13] Schwartz A R, Thut D C, Russ B, Seelagy M, Yuan X, Brower R G, Permutt S, Wise R A and Smith P L 1993 Effect of electrical stimulation of the hypoglossal nerve on airflow mechanics in the isolated upper airway *Am. Rev. Respir. Dis.* **147** 1144–50
- [14] Eisele D W, Schwartz A R, Hari H, Thut D C and Smith P L 1995 The effects of selective nerve stimulation on upper airway airflow mechanics *Arch. Otolaryngol. Head Neck Surg.* **121** 1361–4
- [15] Schwartz A R *et al* 2001 Therapeutic electrical stimulation of the hypoglossal nerve in obstructive sleep apnea *Arch. Otolaryngol. Head Neck Surg.* **127** 1216–23
- [16] Evans H E (ed) 1999 *Miller's Anatomy of the Dog* (Philadelphia, PA: Saunders)
- [17] Mu L and Sanders I 1998 Neuromuscular specializations of the pharyngeal dilator muscles: I. Compartments of the canine genioid muscle *Anat. Rec.* **250** 146–53
- [18] Mu L and Sanders I 1999 Neuromuscular organization of the canine tongue *Anat. Rec.* **256** 412–24
- [19] Mu L and Sanders I 2000 Neuromuscular specializations of the pharyngeal dilator muscles: II. Compartmentalization of the canine genioglossus muscle *Anat. Rec.* **260** 308–25
- [20] Tyler D J and Durand D M 1997 A slowly penetrating interfascicular nerve electrode for selective activation of peripheral nerves *IEEE Trans. Rehabil. Eng.* **5** 51–61
- [21] Yoo P, Sahin M and Durand D M 2004 Selective stimulation of the canine hypoglossal nerve using a multi-contact cuff electrode *Ann. Biomed. Eng.* **32** 511–9
- [22] Sahin M and Durand D M 2000 Selective stimulation of the hypoglossal nerve *Proc. IEEE/EMBS 22th Int. Conf.*
- [23] Tyler D J and Durand D M 2002 Functionally selective peripheral nerve stimulation with a flat interface nerve electrode *IEEE Trans. Neural. Syst. Rehabil. Eng.* **10** 294–303
- [24] Huang J, Sahin M, Noormahammad C and Durand D M 2004 Activation patterns of the tongue muscles with selective stimulation of the hypoglossal nerve *Proc. 26th IEEE/EMBS Conf.*
- [25] Rama A N, Tekwani S H and Kushida C A 2002 Sites of obstruction in obstructive sleep apnea *Chest* **122** 1139–47
- [26] Hwang J C, St John W M and Bartlett D Jr 1983 Respiratory-related hypoglossal nerve activity: influence of anesthetics *J. Appl. Physiol.* **55** 785–92
- [27] Arens R, McDonough J M, Corbin A M, Rubin N K, Carroll M E, Pack A I, Liu J and Udupa J K 2003 Upper airway size analysis by magnetic resonance imaging of children with obstructive sleep apnea syndrome *Am. J. Respir. Crit. Care Med.* **167** 65–70
- [28] Fuller D D, Williams J S, Janssen P L and Fregosi R F 1999 Effect of co-activation of tongue protruder and retractor muscles on tongue movements and pharyngeal airflow mechanics in the rat *J. Physiol.* **519** 601–13
- [29] Miki H, Hida W, Shindoh C, Kikuchi Y, Chonan T, Taguchi O, Inoue H and Takishima T 1989 Effect of electrical stimulation of the genioglossus on upper airway resistance in anesthetized dogs *Am. Rev. Respir. Dis.* **140** 1279–84
- [30] Oliven A *et al* 2003 Upper airway response to electrical stimulation of the genioglossus in obstructive sleep apnea *J. Appl. Physiol.* **95** 2023–9
- [31] Kuna S T 2001 Effects of pharyngeal muscle activation on airway size and configuration *Am. J. Respir. Crit. Care Med.* **164** 1236–41
- [32] Kuna S T 2004 Regional effects of selective pharyngeal muscle activation on airway shape *Am. J. Respir. Crit. Care Med.* **169** 1063–9